

Thermodynamic Water Activity Explains the Unusual Electrochemical Stability of Aqueous Deep Eutectic Solvents

Desiree Mae Prado,^{1,§} Aaron Niño Gonzaga,^{1,§} Brady Carter,² Clemens Burda^{1,}*

¹ Department of Chemistry, Case Western Reserve University, Cleveland, OH 44106, USA

² Novasina AG, 2810 S UT-66, Morgan, UT 84050

[§]Co-first authors, contributed equally to this work

Corresponding Author

^{1,*} Clemens Burda

Department of Chemistry, Case Western Reserve University, Cleveland, OH 44106, USA;

E-mail: burda@case.edu

Abstract

The presence of water in nonaqueous deep eutectic solvent (DES) electrolytes has been debated in recent years, with efforts ranging from its complete removal to willful addition. It was shown that controlled amounts of water can be beneficial, as it not only enhances the physicochemical properties of these electrolytes but also has no significant detrimental effect on their electrochemical stability. Despite these advantages, there is still limited understanding of how water interacts with DES systems at the molecular level. This study examines the water activity in ethylene glycol and glycerol, as well as their binary mixtures with choline chloride to form the DESs ethaline and glyceline, respectively. In this work, we show that the high electrochemical stability of glyceline is related to its lower water activity compared to ethaline and can be attributed to the robust H-bonding network formed by the three hydroxyl groups of glycerol. Its three-dimensional H-bond network effectively integrates water molecules within its solvent structure, reducing degradation and maintaining stability at higher water contents. The deviations from the ideal Raoult's law behavior are reflected in the water activity and activity coefficients, which highlight the intricate hydrogen-bond interactions within DES-water mixtures. Water acts like a lubricant within the more viscous DES mixtures without being detrimental to their electrochemical performance. The presented results emphasize the necessity of customizing DES-water compositions to enhance their performance as electrolytes, especially in flow battery applications where electrochemical stability, ionic conductivity, and fluidity are of utmost importance.

Keywords: water activity, water activity coefficient, deep eutectic solvents, electrochemical stability window, hydrogen bonding

Introduction

Water activity (a_w) is a thermodynamic property that defines the relative chemical potential energy of water and is calculated as the ratio of the equilibrated partial vapor pressure (P_1) of water in the sample to the saturation vapor pressure (P_0) of pure water at the same temperature, $a_w = P_1/P_0$.^[1-4] This concept has been widely used in a wide variety of fields to determine properties such as the microbial growth, enzymatic activity, preservation, and quality of consumer products, including foods and cosmetics.^[5,6] Water activity is extremely important for electrolyte solutions because it describes the solvent—co-solvent (water) interactions.^[7,8] Understanding these interactions is essential to optimizing the performance and longevity of electrolyte systems in various electrochemical technologies, including batteries.

One particularly interesting class of battery solvent systems are deep eutectic solvents (DESs) due to their ability to form intricate networks of H-bonds which enables desirable properties such as low vapor pressure. DESs are multicomponent mixtures formed by combining hydrogen bond acceptors, typically quaternary ammonium salts, with either metal salts or hydrogen bond donors, usually polyalcohols.^[9-11] When mixed in specific molar ratios, these components create solutions with freezing points significantly lower than those of the individual constituents.^[12,13]

Unfortunately, the intermolecular interactions between DES components can also negatively impact the key performance parameters, such as viscosity, conductivity, solubility, and hydrophilicity.^[14-18] These properties can be mitigated by selecting the appropriate types and molar ratios of the selected DES components.^[19-23] Another promising method for tuning DES properties is through controlled hydration.^[24-26] Since DESs are inherently hygroscopic, water can readily ingress into the solvent structure and thereby forming hydrogen bonds with neighboring H-bond donors or acceptors.^[27-33] This hydration process modifies the properties and performance characteristics of the DESs.^[34-38] Understanding how water addition changes these properties is important for designing stable and well performing electrolytes for flow batteries. Knowing the effect of water addition on every aspect of DES characteristics will help optimizing their electrochemical performance for use as alternative green electrolytes in flow batteries.^[19,24,39]

To this end, we examine the water activity and electrochemical stability of ethylene glycol, glycerol, ethaline (a mixture of choline chloride and ethylene glycol in a 1:2 molar ratio)^[9], and glyceline (a mixture of choline chloride and glycerol in a 1:2 molar ratio)^[40] over a range of water concentrations from 0-100 wt. %. We found that the resulting water activity of the two investigated diols is highly sensitive to the addition of choline chloride, while the electrochemical stability depends on the type of H-bond donors present in the DESs. This can be attributed to the specific interactions between the solvent components and water molecules, which influence the overall physicochemical properties of these important solvent systems.

Results and Discussion

The electrochemical stability window (E_w) is affected differently depending on the water content in DESs. **Figure 1** depicts the CV curves of two DES mixtures, ethaline (choline chloride: ethylene glycol, 1:2) and glyceline (choline chloride: glycerol, 1:2), with varying water content. The corresponding cathodic reduction potential limits, anodic oxidation potential limits, and electrochemical stability windows are listed in **Table S5**.

In ethaline, at a water mole fraction of $x_w = 0.18$ (5 wt.%), electrochemical water reduction is evident at a reduction potential of -0.53 V, causing a 4% decrease in E_w , as shown in **Figure 1a**. In contrast, at the same wt. % of water ($x_w = 0.23$) in glyceline (**Figure 1b**), no reduction peak appears, and the decrease in E_w is only 0.9%. The degradation of water in glyceline is not observed until $x_w = 0.80$. At $x_w = 0.92$ in ethaline, the reduction in E_w is 23%, while in glyceline at $x_w = 0.93$, the reduction is 18%. In glyceline, glycerol serves as the primary H-bond donor, contributing to its ability to form a three-dimensional H-bonding network with water. With three -OH groups, glycerol can effectively stabilize water molecules by integrating them into its three-dimensional H-bond network. This structural difference evidently reduces water activity and hinders degradation. This robust H-bonding network in glyceline allows it to tolerate higher water concentrations without significant degradation, making it more stable, while the H-bond donor ethylene glycol provides less protection from the electrochemical degradation of water molecules.

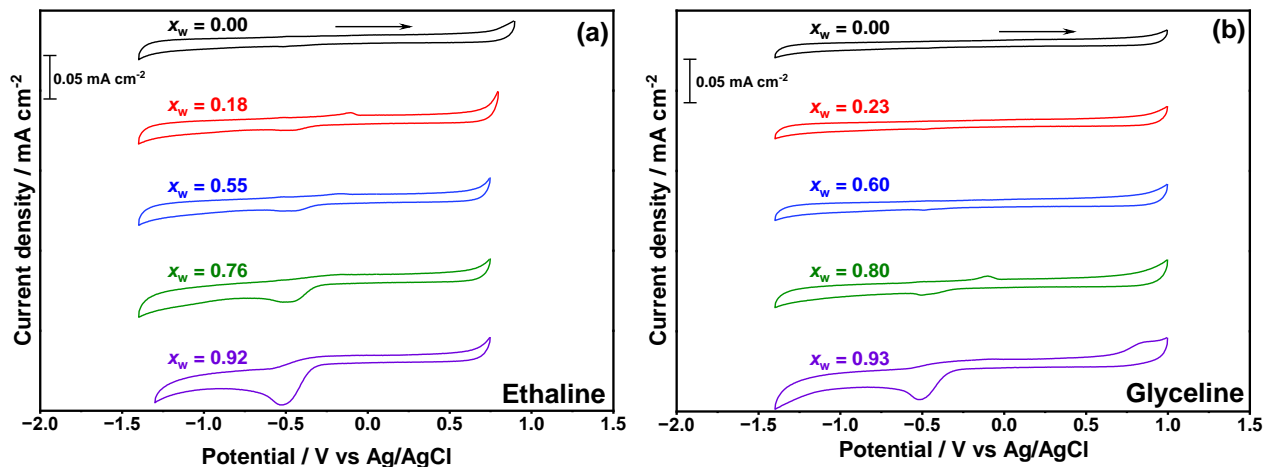


Figure 1. CV curves of DES (a) ethaline (choline chloride: ethylene glycol, 1:2) and (b) glyceline (choline chloride: glycerol, 1:2) with varying water content using GC as working electrode, Pt wire as counter electrode, and Ag/AgCl as reference electrode at a scan rate of 50 mV s^{-1} . The arrow indicates the direction of the scan.

To measure the amount of unbound water available for conversion into hydrogen and oxygen gases during degradation, the water activities of ethylene glycol, glycerol, ethaline, and glyceline were measured. In **Figure 2a**, at low water concentrations, ethaline exhibits more pronounced deviations from the ideal reference line compared to ethylene glycol, which reflects a more complex, nonlinear behavior characteristic of DES-water interactions. As the added water amount is further increased, the water activity of ethaline gradually approaches the ideal reference line more closely. By the time higher water concentrations ($x_w = 0.92$) are reached, the water activity of ethaline is found to be closer to the reference line, suggesting that once enough water has been introduced, the DES-water mixture behaves in a manner that aligns with the classical thermodynamic mixing models like Raoult's law. In ethylene glycol, this transition occurs when water concentration reaches or exceeds $x_w = 0.78$. In **Figure 2b**, the difference between the water activity of glycerol and DES glyceline is marginal. As shown in **Figure 2c**, at $0.2 \leq x_w \leq 0.9$, the water activity of glycerol exhibits greater deviation from the ideal reference line compared to ethylene glycol. In **Figure 2d**, the differences in water activity for ethaline and glyceline become more pronounced at lower water content ($x_w < 0.6$), where glyceline deviates more notably from the reference line compared to ethaline. This indicates that the water activity in glyceline is more effectively 'hidden' relative to ethaline. These observations align with our findings on the

electrochemical stability window in **Figure 1**, where glyceline's three-dimensional hydrogen-bonding network with water makes it less prone to degradation.

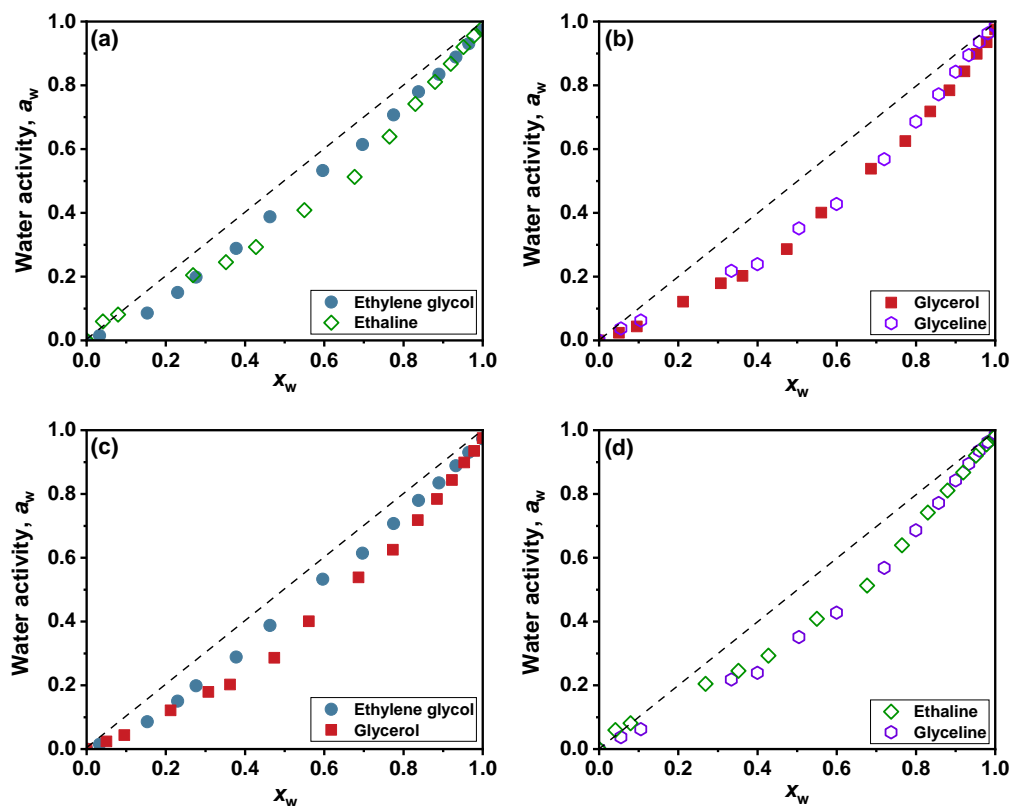


Figure 2. Water activities (a_w) of (a) ethylene glycol (closed circles) vs. ethaline (open diamonds), (b) glycerol (closed squares) vs. glyceline (open hexagons), (c) ethylene glycol (closed circles) vs. glycerol (closed squares), and (d) ethaline (open diamonds) vs. glyceline (open hexagons) with varying mole fractions of water at 25 °C.

In thermodynamics, the activity coefficient (γ_w) is used to determine the non-ideal behavior of a mixture or its deviation from ideality ($\gamma_{\text{ideal}} = 1$) as predicted by Raoult's law. **Figures 3a-d** depicts the comparison of the activity coefficients of different solvents (ethylene glycol, glycerol, ethaline, glyceline). In **Figure 3a**, the activity coefficient of ethaline at $x_w \leq 0.08$ is greater than 1, which means that the interactions between the components in the DES mixture are weaker than the interactions within the pure components, leading to a positive deviation from Raoult's law. At low water content, the activity coefficient of ethaline is higher compared to that of ethylene glycol; however, this trend reverses in the range $0.3 \leq x_w \leq 0.9$.

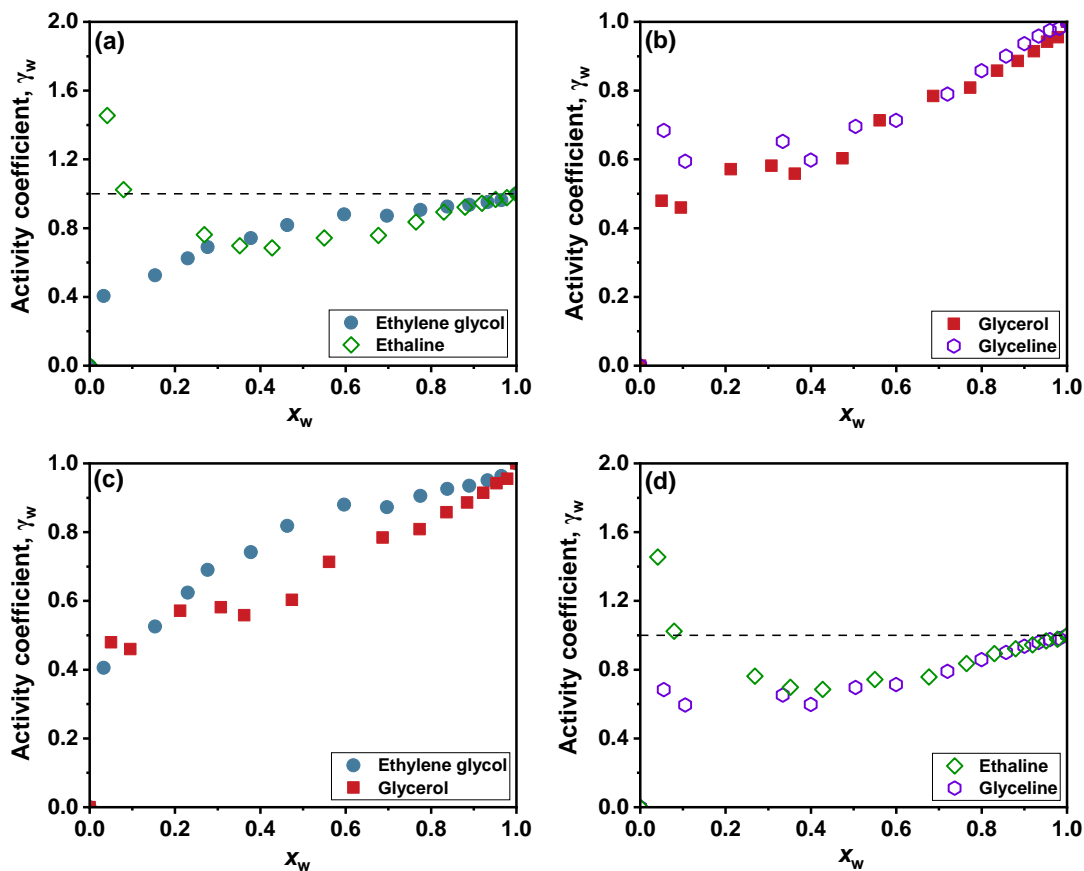


Figure 3. Activity coefficients (γ_w) of (a) ethylene glycol (blue circles) vs. ethaline (open diamonds), (b) glycerol (red squares) vs. glyceline (open purple hexagons), (c) ethylene glycol (blue circles) vs. glycerol (red squares), and (d) ethaline (diamonds) vs. glyceline (hexagons) with varying mole fractions of water at 25 °C.

In **Figure 3b**, the activity coefficients of both glycerol and glyceline decrease with decreasing water content, reaching a minimum at $x_w = 0.10$. Below this mole fraction, both trends reversed. However, the reversal is stronger for glyceline compared to pure glycerol. Glycerol has the lower activity coefficient in the low water content regime, $x_w < 0.20$. This behavior can be attributed to the three-dimensional hydrogen-bonding network in glycerol, which is more affected in the low water concentration range ($0 < x_w < 0.4$), and the activities become more similar as the water content increases. **Figure 3c** demonstrates that glycerol deviates more from ideality than ethylene glycol across the whole range of water contents. Additionally, **Figure 3d** shows that the

differences in activity coefficients between ethaline and glyceline are more pronounced at lower water contents ($x_w < 0.2$), with glyceline exhibiting a greater deviation and lower water activity.

Moisture sorption isotherm describes the relationship between water content (x_w) and water activity (a_w) at a constant temperature. **Figure 4** presents the moisture sorption isotherms of ethylene glycol **(a)**, glycerol **(b)**, and their binary mixtures with choline chloride, forming the DESs ethaline **(c)** and glyceline **(d)**, respectively, at 25 °C.

The moisture sorption isotherms of ethylene glycol and glycerol can be categorized as Type I isotherms due to their rapid initial water sorption at low water content. This behavior is attributed to strong solvent-water interactions, which dominate the adsorption process, especially at low water levels. As the water content increases, the sorption gradually levels off, reflecting the saturation of available adsorption sites.

In contrast, the sorption isotherms for the DESs ethaline and glyceline exhibit characteristics of Type V isotherms. These systems display weak initial water adsorption, as evidenced by the slow rise in sorption at low water content. However, at intermediate water levels, a significant enhancement in water adsorption is observed. This behavior is likely due to changes in the hydrogen-bonding network within the DES, facilitating the incorporation of additional water molecules. This distinction highlights the differences in water sorption mechanisms between individual solvents and DESs, driven by the nature of the solvent-water interactions and the structural properties of the systems.

This is in line with our previously reported results^[23,25,34] that show solvent properties strongly depend on both the composition of the DESs and the structural impact of the interactions between DES components and water molecules. Molecular dynamic simulations of ethaline and glyceline support this interpretation.^[41]

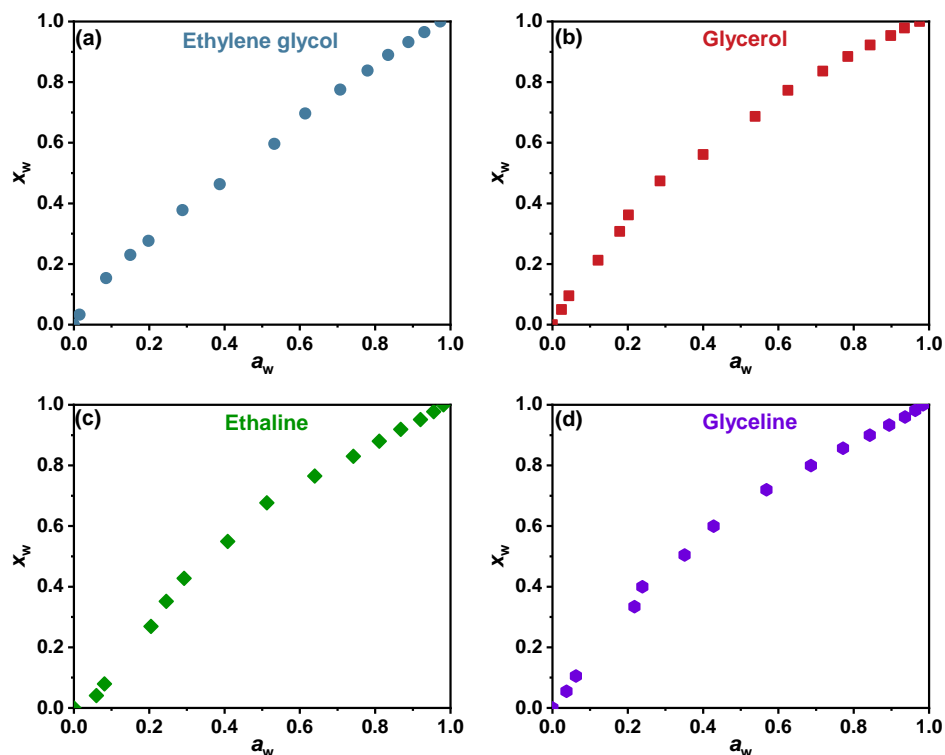


Figure 4. Moisture sorption isotherm of (a) ethylene glycol, (b) glycerol, (c) ethaline (choline chloride: ethylene glycol, 1:2), and (d) glyceline (choline chloride: glycerol, 1:2) at 25 °C. The differences in water sorption between individual solvents (a, b) and DESs (c, d) are most evident in the range of $0.1 \leq a_w \leq 0.5$.

Conclusions

In this study, by examining the electrochemical stability windows of DES-water mixtures, we show that the extent of the stability depends on both the composition of the DESs and the structural impact of the interactions between DES components and water molecules. Wet glyceline, a DES composed of choline chloride and glycerol in 1:2 molar ratio, for example, demonstrates wider electrochemical stability windows compared to the wet DES ethaline (choline chloride: ethylene glycol, 1:2). The enhanced stability of hydrated glyceline at high water content is attributed to its lower water activity due to better ability to integrate water into its hydrogen-bonding network, facilitated by the greater number of hydroxyl groups that form a three-dimensional hydrogen-bond network with the added water molecules.

The deviations from ideality observed in water activity and activity coefficients reflect the non-linear and complex interactions in DES-water mixtures. Also, the moisture sorption behavior of ethylene glycol and glycerol follows Type I isotherms, driven by strong solvent-water interactions, while ethaline and glyceline exhibit Type V isotherms, reflecting weak initial adsorption followed by enhanced water uptake at intermediate water content due to interactions within the DESs. These findings underline the importance of tailoring DES compositions as well as determining and maintaining an optimized water activity level to enhance their performance as electrolytes, particularly in applications such as flow batteries where stability, conductivity, and fluidity are equally important. It is hoped that these results contribute to a deeper understanding of the interactions of deep eutectic solvents and their components with water, which could be an important co-solvent functioning as a lubricant for these otherwise viscous solvent systems. It becomes evident that controlled hydration of DESs can fine-tune and optimize their mechanical properties without leading to their electrochemical breakdown, advancing their potential as electrolyte solutions for future energy storage technologies.

Experimental Section

Chemicals: Ethylene glycol (anhydrous, $\geq 99\%$ purity) and choline chloride ($\geq 99\%$ purity) were purchased from Sigma-Aldrich. Glycerol (99% purity) was obtained from Dot Scientific Inc. Molecular sieves (Type 4Å; 8-12 mesh beads, grade 514) were obtained from Fisher Chemical. To ensure anhydrous conditions, molecular sieves (Type 4Å, 8-12 mesh) were first activated by heating in a furnace at 250 °C for 3 hours to remove residual moisture. After activation, they were placed in contact with the ethylene glycol (EG) and glycerol (G) separately for at least 48 hours, thereby further lowering its water content before use. Choline chloride (ChCl) salt was vacuum-dried at 120 °C for 72 hours prior use. Using a Millipore Milli-Q system, the water added to the samples was purified to a resistivity of 18.2 MΩ cm. The water contents of pure ethylene glycol and pure glycerol were independently determined using Karl Fischer titration to be 508 ppm and 278 ppm, respectively, which is lower than the water content of the as-received chemicals.

Preparation of binary mixtures: DES ethaline was prepared by mixing dried ChCl and dried EG in a 1:2 molar ratio, while DES glyceline was prepared using dried ChCl and dried G in the same molar ratio inside the glovebox under an argon atmosphere. The DES mixtures were then sonicated

at 80°C for 2 hours until a clear solution was obtained, then allowed to cool to room temperature, following the procedure reported in the literature.^[42] Mixtures of solvents (ethaline, glyceline, ethylene glycol, glycerol) with water were prepared by quantitatively adding water to achieve samples containing 0, 1, 2, 5, 8, 10, 15, 20, 30, 40, 50, 60, 70, 80, 90, and 100 wt.% water. The water content of the DESs ethaline and glyceline was determined using Karl Fischer titration (Metrohm Coulometer 899) and found to be below 600 ppm and 300 ppm, respectively.

Cyclic voltammetry measurements: The electrochemical stability window (E_w) of the samples was determined using cyclic voltammetry. CV is performed using a Pine Instruments WaveDriver 200 bipotentiostat and a three-electrode electrochemical cell consisting of a glassy carbon (GC, 3 mm diameter) working electrode, Pt wire counter electrode, and a lab-made Ag/AgCl reference electrode to ensure reliable and accurate potential measurements, as previously reported in the literature.^[43] Briefly, the AgCl film was electrochemically deposited onto a 1.0 mm diameter silver wire (99.9%, Alfa Aesar) using a deposition/stripping square wave method. The silver wire was immersed in a 1 M NaCl electrolyte with a Pt mesh as the cathode. A square wave, applying a +3 mA cm⁻² current for 50 s and a -3 mA cm⁻² current for 2 s, was used. After deposition, the Ag/AgCl wire was rinsed with DI water and dried overnight. The lab-made Ag/AgCl wire was then used as a reference electrode for CV measurements, ensuring that the AgCl-coated portion of the silver wire was submerged in the DES samples. A scan rate of 50 mV s⁻¹ was used for all measurements. The iR compensation was performed before every cyclic voltammetry measurement. Then, E_w was calculated by subtracting the cathodic reduction potential (E_{red}) from the anodic oxidation potential (E_{ox}). Both E_{red} and E_{ox} were identified from the CV curves, where the corresponding potentials were taken at a cutoff current density of ± 0.01 mA cm⁻² for reduction and oxidation processes.

Water activity measurements: Water activity was initially measured following the protocol by Wu, S. et al.^[44] The DES mixtures were placed in a round bottom flask and then a freeze-thaw cycle was performed three times to remove any gaseous impurities from the mixtures. After the last thawing process, the vapor pressure was measured using the MKS Baratron® Type 626D pressure transducer (0.1-1000 Torr) and a two-channel digital power supply and readout. The vapor pressure measurements were time-consuming and highly temperature sensitive. Therefore, we moved to electrolytic a_w measurements using a dedicated water activity meter with temperature calibration, which allowed quicker, and more reliable data collection, as tested with multiple repeat

($n = 3 - 6$) measurements. The two water activity measurement methods were overall consistent and gave similar results.

Consequently, complete sets of water activity (a_w) measurements were conducted using a LabMaster-aw Neo device (Novasina, Sensor ENS/ELS), calibrated for accuracy within $\pm 0.0003 a_w$. Calibration was performed with SAL-T standards at relative humidity (RH) levels of 11%, 33%, 58%, 75%, 84%, 97% and 100% with a tolerance of $\pm 0.0050 a_w$. A filter supplied with the instrument was used during calibration to ensure selectivity for water only.

Prior to each measurement, a regeneration kit was placed in the chamber to perform regeneration cycles, ensuring consistent results and sensor protection. A redox filter was used to safeguard the sensor from exposure to organic volatile compounds. To minimize fluctuations caused by ambient humidity and inadvertent moisture uptake, the water activity measurements were performed inside an inert gas-filled glovebox. The instrument chamber was maintained at a controlled temperature of $25\text{ }^\circ\text{C}$ ($\pm 0.02\text{ }^\circ\text{C}$) throughout the experiments. Each sample was analyzed in triplicate, with the average and standard deviation reported.

Our experimental water activity measurements and calculated activity coefficients of DESs ethaline and glyceline were compared with the data from Wu, S. et al.,^[44] as presented in **Figure S1**. The results show a close agreement. A comparison of water activity and the activity coefficient of glycerol with data from Nakagawa et al.^[45] is also shown in **Figure S2**. The higher water activity and activity coefficients in their data likely result from greater water content in their samples. They did not indicate whether their samples were dried prior to measurement, whereas our results reflect data obtained from dried solvent.

Since commercially purchased solvents inherently contain some water. We have developed experimental drying protocols to minimize water content as much as possible. However, small amounts of water remained even in the driest of our samples. A linear data correction function was applied, primarily at very low water concentrations as follows. To account for this, a subtraction method for water at the 0 wt. % water mark, was employed. This ensured that the data curve goes through the $(0 x_w, 0 a_w)$ and $(1 x_w, 1 a_w)$ points, which are fix points for the thermodynamic ideal mixing functions as shown as a dashed black straight line in **Figure 2** and in **Figures 3a and 3d**. This approach allows to compare our measured water activity data with the ideal thermodynamic

composition based on Raoult's law. For correction functions, see **Tables S1-S4** in the supporting information.

Supporting Information

The authors have cited additional references within the Supporting Information.^[44,45] The Supporting Information includes the water activity, activity coefficient, anodic oxidation potential limits, cathodic reduction potential limits, and electrochemical stability window of pure solvents and DES mixtures as a function of varying mole fraction of water.

Acknowledgments

This work was supported as part of the Breakthrough Electrolytes for Energy Storage and Systems (BEES2), an Energy Frontier Research Center funded by the U.S. Department of Energy, Office of Science, Basic Energy Sciences under Award # DE-SC0019409.

Conflict of Interest

The authors declare no conflict of interest

Data Availability

The data that support the findings of this study are available from the corresponding author upon reasonable request.

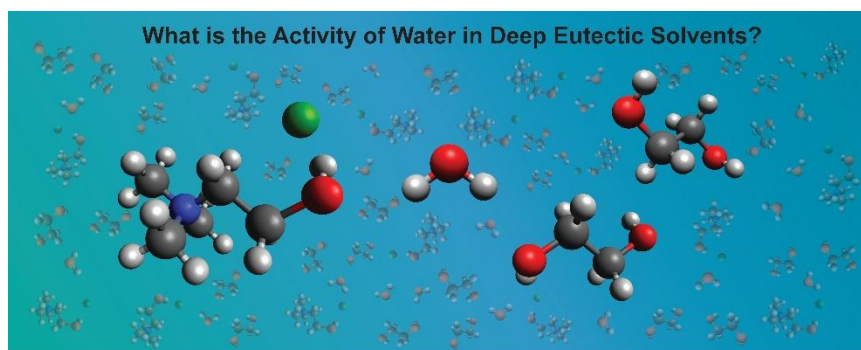
References

- [1] F. M. Raoult, *Compt. Rend.* **1887**, *104*, 1430.
- [2] F. M. Raoult, *Z. Physik. Chem.* **1888**, *2*, 353.
- [3] K. Pitzer, L. Brewer, *Thermodynamics*, 2nd ed., McGraw-Hill, New York, **1961**.
- [4] G. L. Bertrand', C. Treiner, *J Solution Chem* **1984**, *13*.
- [5] W. Scott, *Aust J Biol Sci* **1953**, *6*, 549.
- [6] Y. H. Roos, *J Food Process Preserv* **1993**, *16*, 433.
- [7] Y. Zhigalenok, S. Abdimomyn, M. Levi, N. Shpigel, M. Ryabicheva, M. Lepikhin, A. Galeyeva, F. Malchik, *J Mater Chem A Mater* **2024**, *12*, 33855.

- [8] E. Dutkiewicz, A. Jakubowska, *Journal of Physical Chemistry B* **1999**, *103*, 9898.
- [9] A. P. Abbott, G. Capper, D. L. Davies, H. L. Munro, R. K. Rasheed, V. Tambyrajah, *Chemical Communications* **2001**, *1*, 2010.
- [10] A. P. Abbott, D. Boothby, G. Capper, D. L. Davies, R. K. Rasheed, *J Am Chem Soc* **2004**, *126*, 9142.
- [11] A. P. Abbott, G. Capper, D. L. Davies, R. K. Rasheed, V. Tambyrajah, *Chemical Communications* **2003**, 70.
- [12] B. B. Hansen, S. Spittle, B. Chen, D. Poe, Y. Zhang, J. M. Klein, A. Horton, L. Adhikari, T. Zelovich, B. W. Doherty, B. Gurkan, E. J. Maginn, A. Ragauskas, M. Dadmun, T. A. Zawodzinski, G. A. Baker, M. E. Tuckerman, R. F. Savinell, J. R. Sangoro, *Chem Rev* **2021**, *121*, 1232.
- [13] E. L. Smith, A. P. Abbott, K. S. Ryder, *Chem Rev* **2014**, *114*, 11060.
- [14] A. K. Halder, P. Ambure, Y. Perez-Castillo, M. N. D. S. Cordeiro, *Journal of CO2 Utilization* **2022**, *58*, 101926.
- [15] E. L. Smith, A. P. Abbott, K. S. Ryder, *Chem Rev* **2014**, *114*, 11060.
- [16] Q. Zhang, K. De Oliveira Vigier, S. Royer, F. Jérôme, *Chem Soc Rev* **2012**, *41*, 7108.
- [17] F. Zhen, L. Percevault, L. Paquin, E. Limanton, C. Lagrost, P. Hapiot, *Journal of Physical Chemistry B* **2020**, *124*, 1025.
- [18] K. Shahbaz, F. S. Mjalli, G. Vakili-nezhaad, I. M. Alnashef, A. Asadov, M. M. Farid, *J Mol Liq* **2016**, *222*, 61.
- [19] D. M. Prado, C. Burda, *J Phys Chem Lett* **2024**, *15*, 6343.
- [20] I. Alfurayj, C. Cecilia Fraenza, R. Pandian, S. Greenbaum, C. Burda, *J Mol Liq* **2023**, *392*, 123448.
- [21] I. Alfurayj, R. Pandian, S. Springer, C. Burda, *J Mol Liq* **2023**, *386*, 122454.
- [22] S. Spittle, D. Poe, B. Doherty, C. Kolodziej, L. Heroux, M. A. Haque, H. Squire, T. Cosby, Y. Zhang, C. Fraenza, S. Bhattacharyya, M. Tyagi, J. Peng, R. A. Elgammal, T. Zawodzinski, M. Tuckerman, S. Greenbaum, B. Gurkan, C. Burda, M. Dadmun, E. J. Maginn, J. Sangoro, *Nat Commun* **2022**, *13*, 219.
- [23] X. Shen, N. Sinclair, C. Kellamis, B. Gurkan, J. Wainright, R. Savinell, *J Mol Liq* **2023**, *391*, 123314.
- [24] D. M. Prado, X. Shen, R. Savinell, C. Burda, *Electrochim Acta* **2023**, *467*, 143082.
- [25] I. Alfurayj, C. C. Fraenza, Y. Zhang, R. Pandian, S. Spittle, B. Hansen, W. Dean, B. Gurkan, R. Savinell, S. Greenbaum, E. Maginn, J. Sangoro, C. Burda, *Journal of Physical Chemistry B* **2021**, *125*, 8888.

- [26] I. Alfurayj, D. M. Prado, R. C. Prado, A. C. Samia, C. Burda, *J Phys Chem B* **2024**, *128*, 2762.
- [27] K. Töpfer, A. Pasti, A. Das, S. M. Salehi, L. I. Vazquez-Salazar, D. Rohrbach, T. Feurer, P. Hamm, M. Meuwly, *J Am Chem Soc* **2022**, *144*, 14170.
- [28] Y. Chen, D. Yu, W. Chen, L. Fu, T. Mu, *Physical Chemistry Chemical Physics* **2019**, *21*, 2601.
- [29] M. H. Mamme, S. L. C. Moors, E. A. Mernissi Cherigui, H. Terry, J. Deconinck, J. Ustarroz, F. De Proft, *Nanoscale Adv* **2019**, *1*, 2847.
- [30] J.-D. Wu, Y. Ding, F. Zhu, Y. Gu, W.-W. Wang, L. Sun, B.-W. Mao, J.-W. Yan, *Molecules* **2023**, *28*, 2300.
- [31] O. S. Hammond, D. T. Bowron, K. J. Edler, *Angewandte Chemie - International Edition* **2017**, *56*, 9782.
- [32] C. Du, B. Zhao, X. B. Chen, N. Birbilis, H. Yang, *Sci Rep* **2016**, *6*, 1.
- [33] V. Alizadeh, F. Malberg, A. A. H. Pádua, B. Kirchner, *Journal of Physical Chemistry B* **2020**, *124*, 7433.
- [34] R. Pandian, D. Kim, Y. Zhang, I. Alfurayj, D. M. Prado, E. Maginn, C. Burda, *J Mol Liq* **2024**, *393*, 123534.
- [35] L. Sapir, D. Harries, *J Chem Theory Comput* **2020**, *16*, 3335.
- [36] Y. Dai, G. J. Witkamp, R. Verpoorte, Y. H. Choi, *Food Chem* **2015**, *187*, 14.
- [37] Y. Xie, H. Dong, S. Zhang, X. Lu, X. Ji, *J Chem Eng Data* **2014**, *59*, 3344.
- [38] X. Meng, K. Ballerat-Busserolles, P. Husson, J. M. Andanson, *New Journal of Chemistry* **2016**, *40*, 4492.
- [39] X. Cheng, T. Xuan, L. Wang, *Chemical Engineering Journal* **2024**, *491*, 151936.
- [40] A. P. Abbott, R. C. Harris, K. S. Ryder, C. D'Agostino, L. F. Gladden, M. D. Mantle, *Green Chemistry* **2011**, *13*, 82.
- [41] Y. Zhang, H. Squire, B. Gurkan, E. J. Maginn, *J Chem Eng Data* **2022**, *67*, 1864.
- [42] B. Gurkan, H. Squire, E. Pentzer, *Journal of Physical Chemistry Letters* **2019**, *10*, 7956.
- [43] X. Shen, N. Sinclair, J. Wainright, R. Akolkar, R. F. Savinell, *J Electrochem Soc* **2020**, *167*, 086509.
- [44] S. H. Wu, A. R. Caparanga, R. B. Leron, M. H. Li, *Thermochim Acta* **2012**, *544*, 1.
- [45] H. Nakagawa, T. Oyama, *Front Chem* **2019**, *7*.

Table of Contents (ToC) Entry



This study examines the activity of water in pure solvents and deep eutectic solvents (DESs), its deviation from classical thermodynamic models like Raoult's law, and its impact on electrochemical stability of DESs.